J Math Chem (2011) 49:1384–1415
DOI 10.1007/s10910-011-9831-6

ORIGINAL PAPER

I. Numerical nonlinear analysis: differential methods and optimization applied to chemical reaction rate determination

Christopher G. Jesudason

Received: 1 March 2011 / Accepted: 21 April 2011 / Published online: 12 May 2011

Abstract The primary emphasis of this work on kinetics is to illustrate the a posteriori approach to applied nonlinear analysis, where focus on data may also lead to novel outcomes, as may also be the case with the current a priori tendencies of applied analysis, which relies on axioms or constructs concerning the nature of the observable. Here, methods for the determination of chemical rate constants are developed and discussed utilizing nonlinear analysis which does not require exact knowledge of initial reactant concentrations. These methods are compared with those derived from standard methodology for known chemical reactions studied by eminent kineticists and in one case with a reaction whose initial reactant concentration was in doubt. These gradient methods are shown to be consistent with the standard methods on average, and could readily serve as alternatives for standard conditions and can be used for studies where there are limits or unknowns in the initial conditions, such as in the burgeoning fields of astrophysics and astrochemistry, forensics, archeology and biology where the standard methods are not applicable. All four reactions studied exhibited semi-sinusoidal-like change with reactant concentration change which standard integral methods have not highlighted, and which seems to constitute the observation of a new effect. Reasons based on two mechanisms are given for this observation, and experiments are suggested that can discriminate between these two factors. Although first and second order reactions were investigated here, the method applies to arbitrary fractional orders by polynomial expansion of the rate decay curves where closed form integrated expressions do not exist at present. Integral methods for the above will be investigated next.

C. G. Jesudason (✉)
Department of Chemistry and Center for Theoretical and Computational Physics, University of Malaya, 50603 Kuala Lumpur, Malaysia
e-mail: jesu@um.edu.my; chrysostomg@gmail.com

Keywords Numerical nonlinear analysis · Orthogonal polynomial expansion · Chemical reaction rate law · *a priori* constructs · *a posteriori* rationalization

1 Introduction and methods

Chemical kinetic equations were largely developed with the assumption of rate constant invariance where in particular rate constant determination usually required knowledge of the initial concentrations. A possible reason for this assumption is that the rate constant in elementary fluctuation-dissipation theorem is a "kinetic coefficient" that can be determined statistically [1] assuming that the form of the rate law is known. Examples in applications for special cases abound in science literature e.g. [2,3]. Another possible reason is that the chemical rate constant is actually correlated to a theory of molecular structure of the intermediate and solvent matrix as in the Eyring activated-complex theory [4], where the structure is unique. Last but not least, it was defined *a priori* to be a constant for various empirically based reasons. These kinetic equations do not determine the instantaneous rate constant. Some have attempted to relate the structures derived from mathematics, such as in Harmonic analysis and Fourier expansions to experiment to derive a sequence of rate constants for especially first order processes assuming noise to be a factor for the presence of a group of rate constants [5] by fitting experimental data to the analysis. However, the physical model or concept is not evident in such expositions for a spread of rate constant values. In particular, the spread of values refers to very short time scales, whereas here change over a very large time scale of the order of the duration of the experiment has been detected. Much thought has been made by some workers concerning the nature of the relationship between the sciences and mathematics. Prominent amongst these individuals is Escultura [6], who has focused attention on ambiguous and controversial areas of mathematics [7–12] in addition to contributing to novel qualitative modeling concepts in theoretical physics [13]. Essential to the solution of problems in the natural sciences according to his view is "qualitative" or non-quantitative mathematics that includes abstract mathematical spaces and the search for the laws of nature which are not static and invariant. This methodology explains nature in terms of its laws in contrast to the present methodology of physics that only describes the appearances of nature mathematically. In conventional science such as mathematical physics, problems are solved using existing tools of mathematics and physics. In his methodology a physical theory is devised to provide the solution and is a mathematical system whose axioms are laws of nature and requires the discovery of appropriate laws of nature at the current juncture of time. We wish to highlight another aspect to this line of thought. Rephrasing Escultura, current trends in mathematical applications almost always focuses on the creation of mathematical structures that are considered to mirror physical reality and experimental outcomes, implying that previous experimental data are sufficient for theoretical constructs. Less common are applications in mathematics to analyze experimental data using as closely as possible the operational definition of variables to elucidate the validity or otherwise of theories, and to maintain an open view with regard to possibly newer theoretical constructs. One aspect of the tendency

referred to by Escultura is that it encourages the science of prediction in the natural sciences where sometimes considerable resources are expended in performing experiments to verify and substantiate theories, where data that are extraneous and present an anomaly to the theoretical construct is ignored; error analysis in experiment is a procedure to eliminate data that are out of line with a prevailing theory. The methods developed here are of secondary importance compared to the *a posteriori* analysis of the data and its outcomes; these methods refer to variables which come from the experimental definition. The main thrust of this sequel, therefore, is to put priority on the experimental data as an object of mathematical analysis to construct or suggest theoretical and mathematical structures by recourse to elementary analysis of the defined physical variables. The data from the highly empirical field of chemical kinetics when analyzed and treated in this manner suggests the presence of a new effect; it is therefore suggested here that appropriate and consistent theory can be constructed *a posteriori*, rather than *a priori* which is the current tendency alluded to by at least Escultura. Previous work based on precise simulation data [14] of a bidirectional chemical reaction system in equilibrium involving purely elementary reactions in each direction concluded that the rate constants were a function of species concentration through the defined and determined reactivity coefficients for at least these elementary reactions, which contradicts the operational definition of rate constants (for elementary reactions at least) which are not defined functions of the reactant concentration. The change in the rate constant values with concentration changes in the simulation were ascribed to the changes in the force fields along the reaction pathway [14]. There have been descriptions of such variation in coupled, non-elementary reactions but not for elementary ones. The simulation results motivated this study of analyzing well documented reaction data to monitor possible changes in rate constants during the course of the experimental run. However, there may be other reasons other than that due to the potential fields operating in a reactive system in equilibrium in a real, non-simulated experiment. Inhomogeneities in the reaction medium from the moment of commencement of the reaction might also lead to cross-coupling of forces and fluxes, leading to concentration dependencies; indeed, we conclude that this is the predominant effect, with the changes due to a homogeneous potential field being secondary in nature. Even these ancillary phenomena not due to a homogeneous force field are not normally considered in current theoretical formulations. The possibility that our observations are due to artifacts from instrumental errors or the optimization method is reasoned as unlikely since the experiments were conducted by different groups at very different times with different classes of reactions and they all showed the same trend over long time scales. The secondary motivation of this work is the development of appropriate methods in kinetics consonant with experimental definitions. By focusing on gradients, it is possible to determine both the average and instantaneous rate constants that can monitor changes in the rate constant with concentration changes as suggested by the above theories.

For an elementary reaction

$$\mathrm{A}_1 + \nu_2 \mathrm{A}_2 \cdots \nu_{n_r} \mathrm{A}_{n_r} \rightarrow \text{Products} \tag{1}$$

we define the rate constant k as the factor in the equation

$$\frac{d[\mathrm{A}_1]}{dt} = [\dot{\mathrm{A}}] = -k[\mathrm{Q}] \tag{2}$$

where

$$[Q] = \prod_{i=1}^{n_r} [A_i]^{\nu_i} = l_{A_1 A_2 \ldots A_{n_r}}(t) = l_Q(t)$$

with $l_R(t) = [\mathrm{R}](t)$ in general and $l_A(t) = [\mathrm{A}]_1(t)$ in particular, with the notation $l_{A_1}(t) l_{A_2}(t) \ldots l_{A_{n_r}}(t) = l_Q(t)$. The square brackets denote the concentration of the species, and t is the time parameter. For the above, the order O, which need not be integer is defined as $O = \sum_{i=1}^{n_r} \nu_i$. Clearly, for the above

$$k = -\left\{\frac{d[A_1]}{dt}\right\} \Big/ Q. \tag{3}$$

We determine k here directly by developing various methods of computing average and instantaneous gradients for Eq. (2). In traditional methods, the integrated rate law expression is known for only a handful of integer O values of (2) which also require initial conditions; no such restrictions apply to the current numerical technique. Another class of method that we develop combining numerical differentiation through polynomial expansion and a least squares optimization is as follows.

Define the function $R(k)$ for n datapoints as

$$R(k) = \sum_{i=1}^{n} \left(\frac{dl_A(t_i)}{dt} - k l_Q(t_i))\right)^2. \tag{4}$$

Then,

$$R'(k) = 0 \Rightarrow \sum_{i=1}^{n} \left(\frac{dl_A(t_i)}{dt} - k l_Q(t_i)\right) l_Q(t_i) = 0$$

which therefore implies

$$k = -\frac{\sum_{i=1}^{n} \frac{dl_A(t_i)}{dt} . l_Q(t_i)}{\sum_{i=1}^{n} l_Q^2(t_i)}. \tag{5}$$

Equation (5) does not require iterative methods such as Newton-Raphson's (NR) to determine the rate constant. A variant of the $R(k)$ optimization above is found in Sect. 2.0.5; the reason for the variation is that we optimize over an intergrated expression rather than directly the rate equation (2) such as (25) for the first order rate constant k_1 and (26) for the second order constant k_2. All variants of the above methods will be discussed in sequence in what follows. Most kinetic determinations use logarithmic plots with known initial concentrations, although there have been attempts at integral methods [15–26, and refs. therein] that dispense with the initial concentration. These

standard methods all assume constancy of the rate constant k, and therefore have not inspired methodology that can detect the changes to the rate constant that, according to the detailed results of ref. [14] sheds important information on the activation energy profile changes due to the force fields acting on the reacting species. As mentioned above, there are conceivably many other reasons for variation with time of the rate constants; they include coupling of inhomogeneous temperature field gradients with chemical species fluxes, leading to physical variable inhomogeneities in the reaction cell that modifies the rate of reaction with time. This is discussed after the data is presented in what follows.

There have been detailed and specialized reports and treatises of computational techniques over the many decades but these have been sparse and far between. Wiberg [27, p. 757] has described various more advanced series expansion techniques in conjunction with least squares analysis to derive kinetic data. His use of numerical integration is confined to solving by Runge-Kutta integration a set of coupled equations, such as feature in an enzyme-catalysed reaction [27, p. 771]. Wiberg in turn draws upon the collective efforts collated by De Tar [28,29]. It seems that De Tar's collation anticipates to some degree many of the developments cited above in this work's bibliography. A first order treatment of a chemical reaction given in the program LSKIN1 [28, p. 126] requires data and time intervals that are conformable to the Roseveare-Guggenheim time interval requirement. LSKIN2 [29, p. 3] solves for rate constant and initial concentrations of a second order reaction based on a series expansion of the integrated rate law expression. Here, the curvature would introduce "errors" if a linear expansion were used. For both these methods, the constancy of the rate constant k is a basic assumption, which is not the case here.

Nonlinear analysis (NLA), will be attempted here in preliminary form, in order to compute both the instantaneous and average rate constants. In this approach, we avoid completely the method of equating closed form expressions $F_n(\mathbf{d}, k, x)$ of the integrated rate law expression with polynomial expressions of finite order n such as $P_n = \sum_{i=0}^{n} b_i x^i$ where b_i are coefficients that are derived from a least squares optimization of numerical data of experiments, such as found in the works of Johnson, Maltby, De Tar and several others [17,19,29]. Typically, F_n might represent the concentration or concentration index of one of the reactants and $\mathbf{d}$ the initial reactant concentration and other internal variables and k the rate constant; x is typically the time variable. The method is to equate one to one $(1 \leftrightarrow 1)$ the series expansion of $F_n(x)$ such as $F_n = \sum_{i=0}^{n} a_i x^i$ leading to the identification $(a_i \leftrightarrow b_i)$ for $i \leq n$. The a_i coefficients are all known expressions of the rate constant and initial concentrations and pertinent variables $\mathbf{d}$. Hence if the coefficients b_i are determined by some form of optimization technique, utilizing the $(1 \leftrightarrow 1)$ ansatz implies that by solving various equations involving the coefficients, the rate constant and $\mathbf{d}$ variables might be determined. Qualitatively, one can infer the ambiguity of this ansatz. Suppose F_n is monotonically decreasing (as it must for a unidirectional reaction without reactant replenishment): then for $F_n(x) < a, x > q$ for some q. Clearly for very large x, the influence of the higher powers of x^i for any domain segment $\alpha < x < \beta$ where $x > q$ say will predominate. If P_n were optimized within this range from experimental data, then $b_i \neq a_i \ i \leq n$ since $|b_i|$ would have a larger magnitude to compensate for the lower powers of x_i, $(i \leq n)$. Hence an imposed 1–1 correspondence of $(a_i \leftrightarrow b_i)$

when this is not in fact the case to derive the rate constant k and other kinetic coefficients $\mathbf{d}$ from the known values of a_i and their inter-relationships is inaccurate and might only work for "small" values of $x < r$, where r is an ambiguous number that is not stated and therefore the method is not general. In particular, even if the least squares optimization gives a very good fit to the P_n curve, the fact that $b_i \neq a_i \ i \leq n$ implies that the k and $\mathbf{d}$ variables that depends of the 1–1 relationship cannot be guaranteed to be accurate for larger domain spaces for the P_n optimization since these approximate equations only obtain at very low time or concentration values that cannot be assumed to obtain at the time scales and concentrations of all reactions. The method of De Tar and [17] was applied to the reactions featured here with very poor results. Our method then is to directly compare the experimental data and the gradients derived from the polynomial fit without expanding the integrated expressions and comparing coefficients. We analyze 2 first order reactions and one second order one using data from prominent kineticists. In addition, we select one first order reaction whose initial concentration index is ambiguous utilizing the others as a reference to estimate the likelihood of our result based on NLA; if our analysis concurs with the standard results for the 3 reactions from the literature, then one might be confident that the NLA analysis of the ambiguous reaction is reasonably accurate even if it does not concur with the standard analysis that required the value of the ambiguously determined λ_∞ initial concentration index. Important experiments in science are conducted under uncontrolled conditions, such as in astrochemical reaction rate determinations and photochemical emission spectra in the Mars and Titan atmospheres measured over the decades [30–32]. A similar situation obtains in forensic science and archeology and in biological physiological rate determinations. The basic methods presented here caters for both controlled and uncontrolled initial conditions.

The 3 first order reactions (i)–(iii) and second order reaction (iv) studied are itemized below:

(i) the tert. butyl chloride hydrolysis reaction in ethanol solvent (80% v/v) at 25 °C derived from the Year III teaching laboratory of this University (UM) where the initial concentration, although determined, is ambiguous. Because of time constraints, the inaccurate $\lambda_\infty = 2{,}050\ \mu\mathrm{S\,cm^{-1}}$ for (i) was determined by heating the reaction vessel at the end of the monitoring to 60 °C until there was no apparent change in the conductivity when equilibrated back at 25 °C. Reaction (i) involved 0.3 mL of the reactant which was dissolved in 50 mL of ethanol initially. The reaction was conducted at 25 °C and monitored over time (minutes) by measuring conductivity ($\mu\mathrm{S\ cm^{-1}}$) due to the release of H^+ and Cl^- ions as shown below in (6),

$$C_4H_9Cl + H_2O \xrightarrow{k_a} C_4H_9OH + H^+ + Cl^-. \tag{6}$$

This reaction under various conditions is run as a standard laboratory exercise in physical chemistry at Universities throughout the world.

(ii) the methanolysis of ionized phenyl salicylate derived from the literature [33, Table 7.1, p. 381] with presumably accurate values of both the initial concentration and for all data sets of the kinetic run. Reaction (ii) may be written

$$PS^- + CH_3OH \xrightarrow{k_b} MS^- + PhOH \tag{7}$$

where the rate law is pseudo first-order expressed as

$$\text{rate} = k_b[PS]^- = k_c[CH_3OH][PS^-].$$

The methanol concentration is in excess and is effectively constant for the reaction runs [33, p. 407]. The data for this reaction is given in detail in [33, Table 7.1], conducted at 30 °C where several ionic species are present in the reaction solution from KOH, KCl, and H_2O electrolytes.

(iii) the primarily SN1 substitution reaction [34, Table IX, p. 2071] of tertiary butyl bromide (Bu^tBr) with dilute ethyl alcoholic sodium ethoxide in ethanol solvent where there concurrently occurs an approximately 20% contribution of an E1 elimination reaction. Reaction (iii) may be written

$$CH_3CBr \xrightarrow{\text{SN1}} \text{Products} \tag{8}$$

where the solvent was EtOH with initial sodium ethoxide concentration [NaOEt] = 0.02386N at 25 °C. The products consisted of approximately 81% substituted tertiary butyl ethoxide and 19% olefinic molecules due to E1 elimination. Hence the rate constant here refers to a composite reaction (details in [34, p. 2070] and [35, p. 2064]).

(iv) the second order E2 elimination reaction [35, p. 2059–2060 and Table VII, p. 2064] with reactants isopropyl bromide (Pr^iBr) and sodium ethoxide (NaOEt). Reaction (iv) involving isopropyl bromide $Pr^iBr \equiv (CH_3)CHBr(CH_3)$ may be written

$$(CH_3)CHBr(CH_3) + OEt^- \xrightarrow{\text{E2}} CH_2CHCH_3 + Br^- + HOEt \tag{9}$$

where the isopropyl bromide reacts with the OEt^- ion in EtOH solvent at 25°C to yield 80.3% of the olefinic product with some SN2 substitution with the (OEt) functional group [35, Table III, p. 2061] according to the kineticists. Further details and data appear [35, Table VII, p. 2064]. It should be mentioned that the E2 reaction was inferred to be second order from prior experimental considerations since the [NaOEt] concentration reduction from the data exactly coincides with the reduction of Pr^iBr and was not independently determined. Although this type of measurement is perfectly acceptable for the standard integrated expression, NLA is able to detect the scatter due to the larger inaccuracy of the non-cancellation of errors in terms of the non-smooth nature of the instantaneous rate constant curve discussed later (see Fig. 1 for the graph).

"Units" in the figures and text pertain to the appropriate reaction variable dimension, for instance either the conductivity ($\mu S\ cm^{-1}$) for reaction (i) or the light absorbance for (ii) which has no true units. Either because of evaporation or the temperatures not equilibrating after heating, the measured λ_∞ for reaction (i) is larger than the

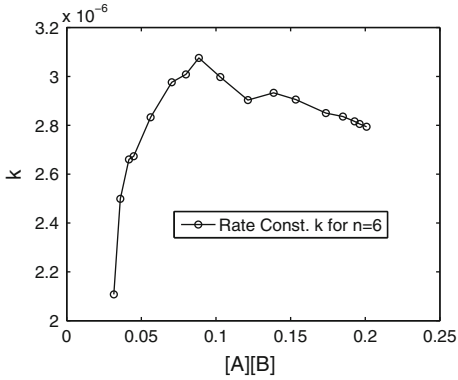

Fig. 1 The computation of the instantaneous rate for reaction (iv) for polynomial fit with $n = 6$ along the regime of coincidence of the polynomials with degrees n =4–7

actual one determined from NLA. Reaction (ii) is very rapid compared to (i) and the experimental data plots show high nonlinearity. We denote by λ the measurement parameter which is the conductivity μS cm^{-1} or absorbance A [33, Eqs. 7.24–7.26] for reactions (i) and (ii) respectively; λ also refers to the concentration [X] of species X for reactions (iii) and (iv). The more accurately determined $\lambda_\infty (= A_\infty)$ for (ii) [33, Table 7.1, p. 381] was at approximately 0.897. Analysis of (ii) give values of A_∞ very close to the experimental ones that suggests that our independent determination for reaction (i) λ_∞ is correct. The experimental data and number of readings for the determination of rate constants is always related to the method used and the order of accuracy required in the study; for Khan [33, Table 7.1, first A column], (reaction (ii)) , 14 normal readings over 360 s sufficed for Khan's purposes, whereas for the practical class (reaction (i)), 36 readings over 55 min were taken. The meager 14 readings of (ii) covered a major portion of the nonlinear region of the reaction, whereas for (i) the many readings were confined to the near-linear regime. Linear proportionality is assumed between λ and the extent of reaction x, where the first order law (c being the instantaneous concentration, k the general rate constant and a the initial concentration) is $\frac{dc}{dt} = -kc = -k(a - x)$; with $\lambda_\infty = \alpha a$, $\lambda_t = \alpha x$ and $\lambda(0) = \lambda_0 = \alpha x_0$, integration yields for assumed constant k

$$\ln \frac{(\lambda_\infty - \lambda_0)}{(\lambda_\infty - \lambda(t))} = kt \tag{10}$$

Equation (10) determines k if λ_0 and λ_∞ are known.

The analysis of well studied reactions (ii)–(iv) would provide a reference and indication of the predicted value in (i) for the initial concentration, apart from checking for overall consistency of the methodology in general situations especially when there is doubt concerning the value of the initial concentration.

The methods presented here applies to any order provided the expressions can be expanded as an n-order polynomial of the concentration variable against the time independent variable. To get smooth curves that are stable one had to modify and use a proper curve-interpolation technique that is stable which does not form sudden kinks or points of inflexion and this follows next.

1.1 Orthogonal polynomial stabilization

It was discovered that the usual least squares polynomial method using Gaussian elimination [36, Sect. 6.2.4, p. 318] to derive the coefficients of the polynomial was highly unstable for $n > 4$, which is a known condition [36, p. 318, Sect. 6.2.4]. For higher orders, there is in addition the tendency to form kinks and loops in an interpolated curve for values between two known intervals. Other methods described in specialized treatises [37, Chap. 5, Sect. 5.7–5.13], even if robust and stable,such as the Chebyshev approximation required values of the proposed experimental curve at predetermined definite points in time, which is outside the control of one using predetermined data and so for this work, the least square approximation was stabilized by orthogonal polynomials [36, Sect.6.3] modified for determination of differentials. The method can also be extended to integrals and results follow in the next sequel. The usual method defines the nth order polynomial $p_n(t)$ which is then expressed as a sum of square terms over the domain of measurement to yield Q_f in (11):

$$\begin{aligned} p_n(t) &= \sum_{j=0}^{n} h_j t^j \\ Q_f(f, p_n) &= \sum_{i=1}^{N} [f_i - p_n(t_i)]^2. \end{aligned} \tag{11}$$

The Q_f function is minimized over the polynomial coefficient space. In the orthogonal method adopted here, we express our polynomial expression $p_m(t)$ linearly in coefficients a_j of φ_j functions that are orthogonal with respect to an *inner* product definition. For arbitrary functions f, g, the inner product (f, g) is defined below, together with properties of the φ_j orthogonal polynomials:

$$\begin{aligned} (f, g) &= \sum_{k=1}^{N} f(t_k) \cdot g(t_k) \\ (\varphi_i, \varphi_j) &= 0\,(i \neq j) \text{ and } (\varphi_i, \varphi_i) \neq 0. \\ \varphi_i(t) &= (t - b_i)\varphi_{i-1}(t) - c_i\varphi_{i-2}(t)\,(i \geq 1), \\ \varphi_0(t) &= 1, \text{ and } \varphi_j = 0 \text{ for } \quad j < 1, \end{aligned} \tag{12}$$

$$\begin{aligned} b_i &= (t\varphi_{i-1}, \varphi_{i-1})/(\varphi_{i-1}, \varphi_{i-1})\ (i \geq 1), \quad b_i = 0\,(i < 1), \\ c_i &= (t\varphi_{i-1}, \varphi_{i-2})/(\varphi_{i-2}, \varphi_{i-2})\ (i \geq 2), \quad \text{and } c_i = 0\ (i < 2). \end{aligned} \tag{13}$$

We define the mth order polynomial and associated a_j coefficients as follows:

$$\begin{aligned} p_m(t) &= \sum_{j=0}^{m} a_j \varphi_j(t), \\ a_j &= (f, \varphi_j)/(\varphi_j, \varphi_j), \quad (j = 0, 1, \ldots m). \end{aligned} \tag{14}$$

The recursive definitions for the first and second derivatives are given respectively as:

$$\varphi_i'(t) = \varphi_{i-1}'(t)(t - b_i) + \varphi_{i-1}(t) - c_i\varphi_{i-2}'(t), \quad (i \geq 1)$$
$$\varphi_i''(t) = \varphi_{i-1}''(t)(t - b_i) + 2\varphi_{i-1}'(t) - c_i\varphi_{i-2}''(t), \quad (i \geq 2) \tag{15}$$

Here the codes were developed in C/C++ which provides for recursive functions which we exploited for the evaluation of all the terms. The experimental data were fitted to an mth order expression $\lambda_m(t)$ defined below

$$\lambda_m(t) = \sum_{j=0}^{m} h_j t^j = p_m(t) = \sum_{j=0}^{m} a_j \varphi_j(t) \tag{16}$$

The coefficients h_j are all computed recursively, and the derivatives determined from (16) or from (14) and (15). Once h_j or a_j are determined, then the gradient to the curve $\lambda_m(t)$ is computed as

$$\lambda_m'(t) = \sum_{j=0}^{m} j h_j t^{j-1}. \tag{17}$$

The $l_Q(t)$ function of (2) is expanded similarly as for $\lambda_m(t)$ for order m. The orthogonal polynomial method is stable and the mean square error decreases with higher polynomial order in general monotonically (where n is used to denote the integer order), but the differentials are not so stable, because of the contribution of higher order coefficients in the differential expression as will be shown. From the form of the of the equation that will be developed, the rate constant is determined as the gradient of a straight-line graph in the appropriate segment of the graph. However, the curvature of the plot will increase with increasing n, giving a poorer value of k, whereas higher values of n would better fit the λ versus t curve. Hence inspection of the plots is necessary to decide on the appropriate n value, where we choose the lowest n value for the most linear graph of the expression under consideration that also provides a good $\lambda(t)$ fit over a suitable time range over which the k rate constants apply. The orthogonal polynomial stabilization method provides good λ fits with increasing n, but not gradients, so that the onset of sudden changes to the gradient which on physical grounds is unreasonable can be used as an indication as to which curve to select. There is in practice little ambiguity in selecting the appropriate polynomials, as will be demonstrated. Reactions (i) and (ii) both gauge initial concentrations in terms of the A_∞ (λ_∞) or final reading of a physical factor proportional to concentration and the structure of the analysis is the same and will therefore be discussed simultaneously, followed by reactions (iii)–(iv), where concentrations are measured directly during the course of the reaction, which will be discussed together because the form of the boundary conditions and data are of the same class.

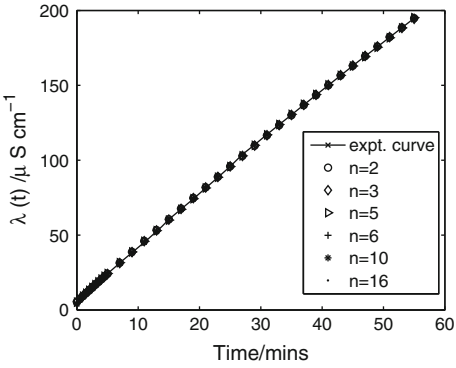

Fig. 2 Plot of data from reaction (i) using orthogonal polynomials for various orders n. The the least squares deviation goes down dramatically with increasing n, which was found not to be the case with the normal non-orthogonal polynomial method

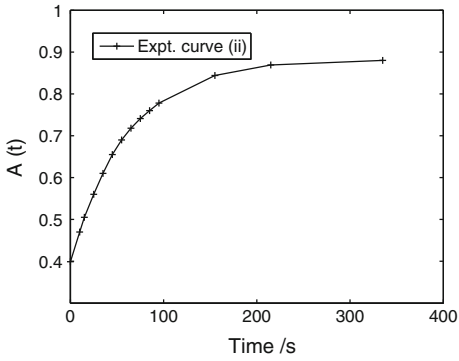

Fig. 3 Experimental points omitting point at A_∞ for reaction (ii) at time = 2,135 s. The *curve* is rather non-linear

2 Analysis of reactions (i) and (ii)

In this section, the rate constant for reaction (i) is denoted k_a and that of reaction (ii) as k_b.

Figure 2 are plots for the different polynomial orders n for reaction (i). It will be noticed that higher n values in general leads to better fits visually; the normal least squares method leads to severe kinks and loop formation for $\sim n \geq 4$ which is not evident here. The reaction (ii) data covers a far greater domain with respect to half-lifetimes with only about 14 points (which is a poor dataset with respect to our methods but which still gives quantitatively accurate values); because of the relatively more rapid curvature changes, we would expect very different gradient behavior as compared to (i) with its stronger linearity.

The corresponding plots for reaction (ii) are in Fig. 3.

In view of the nonlinearity, we chose a limited regime to curve fit for polynomial order $n = 3, 4, 5$ in Fig. 3.The fit for this region is given in Fig. 4 in this reaction (ii). The gradient was computed for the $n = 5$ polynomial to determine the rate constants as it was the only order that gave a smooth curve for the first 12 consecutive points in the range; the other orders also gave consistent and almost equal gradients except at the extreme end points of the range plotted as depicted for example in Figs. 5, 6, 7.

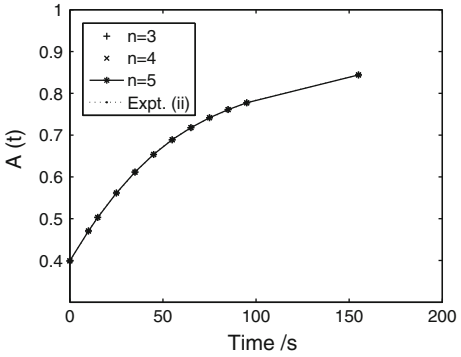

Fig. 4 Experimental points *curve* fitted with polynomials of order $n = 3, 4, 5$. The fit for this range is excellent, despite the nonlinear nature of the *curve*

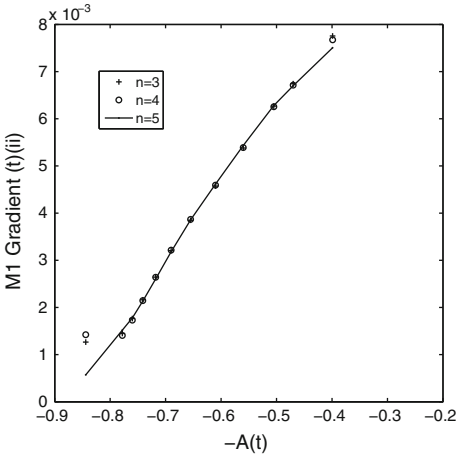

Fig. 5 Method 1 applied to reaction (ii). Only at the peripheral value does the fit fail for lower values of n due to the extreme curvature

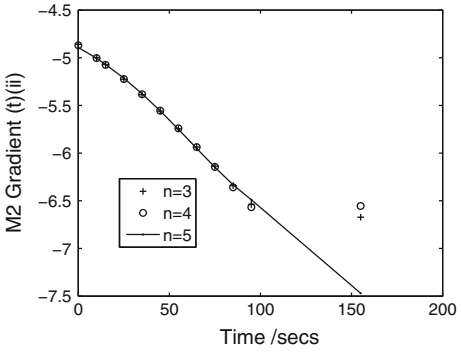

Fig. 6 Method 2 reaction (ii) where smooth *curves* are obtained for $n < 5$. The $n = 5$ polynomial is used to calculate the best linear line over this range as the other polynomials do not fit for the last value in the series due to the extreme curvature

Unlike reaction (ii), the λ_∞ for reaction (i) was ambiguous. The plot of (10) was made for the same experimental values with different λ_∞'s, both higher and lower than the supposed experimental value for this reaction. The plots in Fig. 8 shows increasing

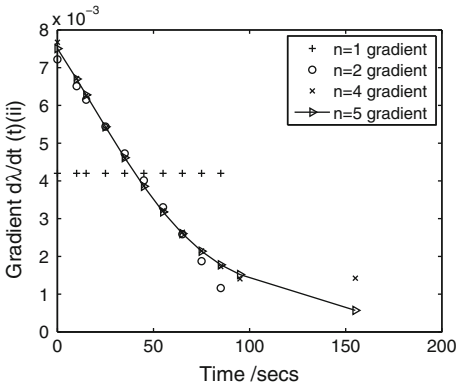

Fig. 7 Variation of gradient $d\lambda = dt = dA/dt$ with time for different polynomial orders $n = 1, 2, 4$ and 5

k_a for decreasing λ_∞; the choice λ_∞ =1,050 leads to a value of k_a close to the NLA values for the different methods discussed which does not require λ_∞, but NLA is also able to determine this value once k_a is determined. The rate constant from NLA is higher than that determined from experiment, implying a lower λ_∞ value which is consonant with evaporation of solvent and/or the non-equilibration of temperature prior to measurement to determine λ_∞. Hence elementary NLA allows one to deduce the accuracy of the actual experimental methodology in this example. Except for one section, we shall apply NLA based on constant k assumption. We also quote some values of Khan's results [33, Table 7.1] in Table 1, where some comment is required. The A absorbance is monotonically increasing and at higher time (t) values (see [33, Table 7.1]) the experimental A value exceeds the A_∞ that is determined by the process of minimizing $\sum d_i^2$. Hence the minimization of $\sum d_i^2$ with respect to A_∞ is taken as a protocol for determining the best k value even if it contradicts experimental observation. Further, this protocol is highly sensitive to A; a change of 10^{-3} leads to an approximately tenfold change in k. On the other hand, if A_∞ determined from experiment as 0.897 is accepted, then then computed rate constant for this value is $k = 2.69 \times 10^{-3}\text{s}^{-1}$ implying that the uncertainty in k is of the order of $\pm 14 \times 10^{-3}$. Hence we can conclude that the Khan method is a protocol that accepts as correct the k value that is determined by the minimization of A_∞ for a certain A_∞ range ($\approx$0.8980 to.8805), which again refers to an unspecified protocol as to the choice of the range.

2.0.1 Method 1

This method is a variant of the direct method of Eq. (2). For constant k, the rate equation $\frac{dc}{dt} = -kc = -k(a - x)$ reduces to

$$\frac{\lambda(t)}{dt} = -k\lambda(t) + \lambda_\infty k \tag{18}$$

Hence a plot of $\frac{\lambda(t)}{dt}$ versus $\lambda(t)$ would be linear. We find this to be the case for polynomial order $n \leq 3$ as in Fig. 9 below for all data values; higher polynomial orders can be used in selected data points of the curve below, especially in the central region.

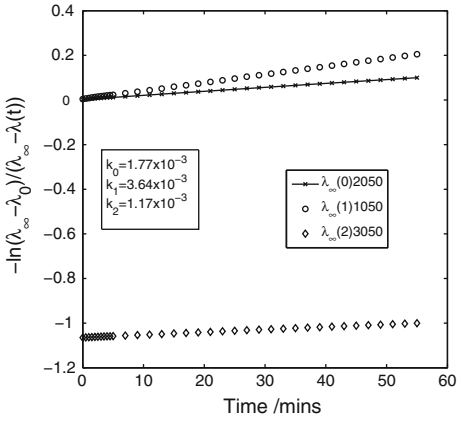

Fig. 8 Integrated equation (10) plot with λ_∞ from experiment (with subscript 0) and from two different arbitrary values (1, 2) for λ_∞, which yields two different values for the rate constant (subscripted 1 and 2, respectively) due to gradient change

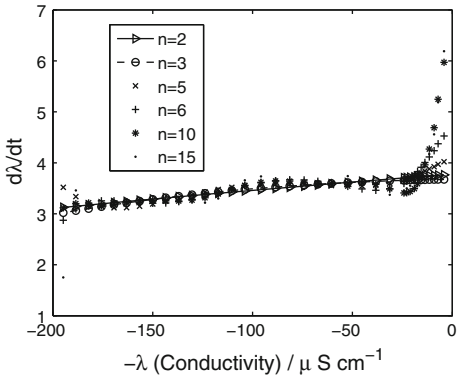

Fig. 9 Method 1 graph showing linearity lower order polynomial fits for reaction (i)

Thus criteria must be set up to determine the appropriate regime of data points for a particular polynomial order in NLA. For $n = 2$, $k_a = 3.34 \pm .03 \times 10^{-3}\text{min}^{-1}$ and $\lambda_\infty = 1{,}134 \pm 10$ units. The plots for reaction (ii) is a little more involved; it is a much more rapid reaction and the number of data-points are relatively sparse for NLA and the points cover the entire range of the reaction sequence and is highly non-linear; it was found that the gradients were smooth for the first 10 or so points and reasonably linear, but that at the boundary of these selected points, there are deflections in the curve; on the other hand, the different polynomial order curves ($n \leq 5$) are all coincident over a significant range of these values; we chose the $n = 5$ polynomial curve (Fig. 5) to determine the curve over the entire range and the linear least squares fit yields the following data $k_b = 1.64 \pm .04 \times 10^{-2}\text{s}^{-1}$ and $A_\infty = 0.8787 \pm .0008$ units.

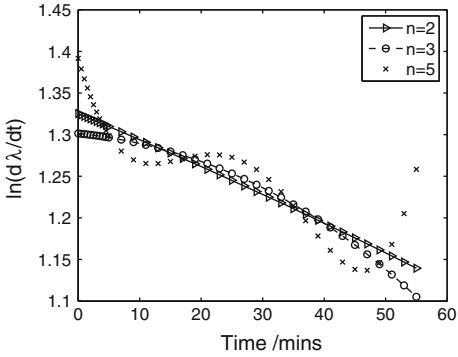

Fig. 10 Method 2 reaction (i) where smooth *curves* are obtained for at least $n < 4$

2.0.2 Method 2

This method is yet another variant of the direct method of Eq. (2). Let $\alpha' = \lambda_\infty - \lambda_0$, then $\ln \alpha' - \ln(\lambda_\infty - \lambda) = kt$, then noting this and differentiating yields

$$\ln\left(\frac{d\lambda}{dt}\right) = -kt + \ln[k(\lambda_\infty - \lambda_0)] \tag{19}$$

which is of the linear form $Y = Mt + C$.

A typical plot that can extract k as a linear plot of $\ln(d\lambda/dt)$ versus t is given in Fig. 10 for Method 2, reaction (i) and in Fig. 6 for Method 2, reaction (ii). Linearity is observed for $n = 2$ and smooth curves without oscillations for at least $n \leq 3$ for reaction (i) and an analysis for reaction (ii) uses $n = 5$. The linear least square line yields for Method 2 the following:

$$k_a = 3.35 \pm .03 \times 10^{-3}\text{min}^{-1} \text{ and } \lambda_\infty = 1,130 \pm 10 \text{ units}$$
$$k_b = 1.72 \pm .02 \times 10^{-2}\text{s}^{-1} \text{ and } A_\infty = 0.86(53) \pm .02 \text{ units}.$$

We note that because of the manifest nonlinearly of the gradients, one cannot in our method determine the A_∞ values to 4-decimal place accuracy as quoted by Khan based on his model and assumptions [33, Table 7.1], such as the invariance of the rate constant.

2.0.3 Other associated non-direct methods

There are other methods, one of which is a variant of Method 1 and another that utilizes a least-squares optimization of the form of the equation for first and second derivatives.

2.0.4 Method 1 variation

A variant method similar to the Guggenheim method [16] of elimination is given below but where gradients to the conductivity curve is required, and where the average over all pairs is required; the equation follows from (19).

$$\langle k \rangle = \frac{-2}{N(N-1)} \sum_{i}^{N} \sum_{j>i}^{N} \ln\left(\lambda'(t_i)/\lambda'(t_j)\right)/(t_i - t_j) \tag{20}$$

Since we are averaging over instantaneous k values, there would be a noticeable standard deviation in the results if the hypothesis of change of rate constant with species concentration is correct. Differentiating (19) for constant k leads to (21) expressed in two ways

$$\frac{d^2\lambda}{dt^2} = -k\left(\frac{d\lambda}{dt}\right)(a) \text{ or } k = -\frac{d^2\lambda}{dt^2}/\left(\frac{d\lambda}{dt}\right)(b) \tag{21}$$

If $\lambda(t) = \sum_{i=0}^{n+1} a(i)t^{i-1}$, then as $t \to 0$, the rate constant is given by $k = \frac{-2a(2)}{a(1)}$ from (21b). For the above, $n, id,$ and iu denotes as usual the polynomial degree, the lower coordinate index and the upper index of consecutive coordinate points respectively, where the average is over the consecutive points, whereas the k rate constant with subscript "all" below refers to the Eq. (20).

The results from this calculation are as follows:

$$\begin{aligned} k_{a,all}, k_{a,id,iu} &= 3.32, 3.23 \pm .07 \times 10^{-3}\,\text{min}^{-1},\ n = 2, id = 10, iu = 20 \\ k_{a,t\to 0} &= 3.082 \times 10^{-3}\text{min}^{-1}. \\ k_{b,all}, k_{b,id,iu} &= 1.7150, 1.676 \pm .3 \times 10^{-2}\,\text{s}^{-1},\ n = 5, id = 1, iu = 10 \\ k_{b,t\to 0} &= 1.023 \times 10^{-2}\text{s}^{-1}. \end{aligned}$$

The asymptotic limit gives a lower value for k_b than for the other methods for reactions (i) and (ii). One possible explanation is that the rate constant changes as a function of time, but we note that (21) was derived assuming constant k.

2.0.5 Optimization of first and second derivative expressions

Equation (21b) suggests another way of computing k for "well-behaved" values of the differentials, meaning regions where k would appear to be a reasonable constant. The (a) form of (21) suggests an exponential solution. Define $\frac{d\lambda}{dt} \equiv dl$ and $\frac{d^2\lambda}{dt^2} \equiv d2l$. Then $dl(t) = A\exp(-kt)$ and $dl(0) = A = h_2$ from (16). Furthermore, as $t \to 0$, $k = (-2h_2/h_1)$ and a global definition of the rate constant becomes possible based on the total system $\lambda(t)$ curve.

With a slight change of notation, we now define dl and $d2l$ as referring to the continuous functions $dl(t) = A\exp(-kt)$ and $d2l(t) = -kA\exp(-kt)$ and we consider $(d\lambda/dt)$ and $d^2\lambda/dt^2$ to belong to the values (16) derived from ls fitting where

$(d\lambda/dt) = \lambda'_m$, $(d^2\lambda/dt^2) = \lambda''_m$ which are the experimental values for a curve fit of order m. From the experimentally derived gradients and differentials, we can therefore define two non-negative functions $R_\alpha(k)$ and $R_\beta(k)$ as below:

$$R_\alpha(k) = \sum_{i=1}^{N} \left(\frac{d^2\lambda(t_i)}{dt^2} + kdl(t_i) \right)^2$$
$$R_\beta(k) = \sum_{i=1}^{N} \left(\frac{d\lambda(t_i)}{dt} - dl(t_i) \right)^2 \tag{22}$$

where $f_\alpha(k) = R'_\alpha(k)$ and $f_\beta(k) = R'_\beta(k)$ and a stationary point (minimum) exists at $f_\alpha(k) = f_\beta(k) = 0$. We solve the equations f_α, f_β for their roots in k using the Newton-Raphson method to compute the roots as the rate constants k_α and k_β for functions $f_\alpha(k)$ and $f_\beta(k)$, respectively. The error threshold in the Newton-Raphson method was set at $\epsilon = 1.0 \times 10^{-7}$ We provide a series of data of the form $[n, A, k_\alpha, k_\beta, \lambda_{\alpha,\infty}, \lambda_{\beta,\infty}]$ where n refers to the polynomial degree, A the initial value constant as above, k_α and k_β are the rate constants for the functions f_α and f_β (solved when the functions are zero respectively) and likewise for $\lambda_{\alpha,\infty}$ and $\lambda_{\beta,\infty}$. The λ_∞ values are averaged over all the 36 data points for reaction (i) and for the 12 datapoints of reaction (ii) from the equation

$$\lambda_\infty = \frac{d\lambda(t)}{dt}\frac{1}{k} + \lambda(t) \tag{23}$$

for scheme α and β for both reaction (i) and (ii). The results are as follows.

Reaction (i)

$[2, 3.7632 \times 10^0, 3.2876 \times 10^{-3}, 3.2967 \times 10^{-3}, 1.1506 \times 10^3, 1.1477 \times 10^3]$,
$[3, 3.6384 \times 10^0, 2.7537 \times 10^{-3}, 2.7849 \times 10^{-3}, 1.34756 \times 10^3, 1.3334 \times 10^3]$,
$[4, 3.6384 \times 10^0, 2.0973 \times 10^{-3}, 2.4716 \times 10^{-3}, 1.7408 \times 10^3, 1.4900 \times 10^3]$,
$[5, 4.0213 \times 10^0, 9.7622 \times 10^{-3}, 4.9932 \times 10^{-3}, 4.4709 \times 10^2, 7.9328 \times 10^2,]$,
$[6, 4.5260 \times 10^0, 4.1270 \times 10^{-2}, 8.9257 \times 10^{-3}, 1.7101 \times 10^2, 4.8403 \times 10^2]$.

We noticed as in the previous cases that the most linear values occur for $1 < n < 4$. In this approach, we can use the f_α and f_β function similarity of solution for k_α and k_β to determine the appropriate regime for a reasonable solution. Here, we notice a sudden departure of similar value between k_α and k_β (about 0.4 difference) at $n = 4$ and so we conclude that the probable average "rate constant" is about the range given by the values spanning $n = 2$ and $n = 3$. Interestingly, the λ_∞ values are approximately similar to the ones for Method 1 and 2 for polynomial order 2 and 3 for reaction (i). More study with reliable data needs to be done in order to discern and select appropriate criteria that can be applied to these non-linear methods. Because of the large number of datapoints in the linear range, k_α and k_β values are very compatible for $n = 2, 3$ where the k_α determination involves double derivatives, which cannot be determined with accuracy unless a sufficient number of points is used.

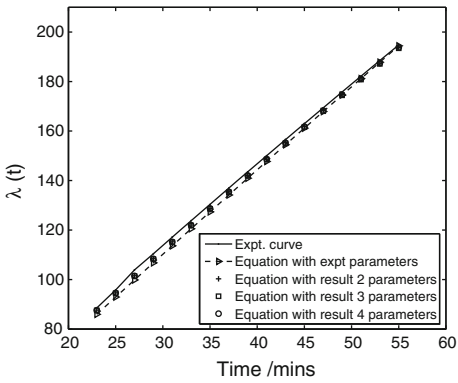

Fig. 11 The plots according to the k_i and λ_∞ values of Table 2 for reaction (i). The plot with the parameters derived through the ambiguously determined experimental λ_∞ is the poorer fit compared to the NLA fits

Reaction (ii)
The results for this system are

$$\left[5, 7.5045 \times 10^{-3}, 1.2855 \times 10^{-2}, 1.5497 \times 10^{-2}, .94352, .89247\right]$$

for the first 12 datapoints of the published data to time coordinate 155 s. For polynomial order 3,4 and the first 11 datapoints, where there are no singularities in the curve we have

$$\left[3, 7.7275 \times 10^{-3}, 1.4469 \times 10^{-2}, 1.6147 \times 10^{-2}, .91320, .88335\right]$$
$$\left[4, 7.4989 \times 10^{-3}, 1.3146 \times 10^{-2}, 1.5359 \times 10^{-2}, .94208, .89652\right].$$

Here, k_α and k_β differ by $\sim .2 \times 10^2\ \mathrm{s}^{-1}$ for all the n polynomial orders; one possible reason for this discrepancy is the insufficient number of datapoints to to accurately determine $\frac{d^2\lambda}{dt^2}$. Even if the number of points are large, experimental fluctuations would induce changes in the second derivative which would be one reason for discrepancies. Hence experimentalists who wish to employ NLA must provide more experimental points, especially at the linear region of the $\lambda(t)$ versus t curve.

2.1 Inverse calculation

Rarely are experimental curves compared with the ones that must obtain from the kinetic calculations. Since the kinetic data is the ultimate basis for deciding on values of the kinetic parameters, replotting the curves with the calculated parameters to obtain the most fitting curve to experiment would serve as one method to determine the best method amongst several. For reaction (i) we have the following data in Table 2 used in the plot of Fig. 11:

For reaction (ii), we use the data in Table 3 to plot Fig. 12.

Figure 11 indicate that the parameters derived from experiment is the worst fit compared to the methods developed here, verifying that our computations, including the λ_∞ values are a better fit than the one derived from experiment due to flaws in the methodology of driving the reaction to completion by heating, leading to evaporation and therefore inaccurate determination. Based on the comparisons between

Table 1 Some results from reaction (ii) [33, p. 381, Table 7.1]

$10^3 \sum d_i^2$	513.5	109.4	8.563	63.26	212.7	227.4
A_∞	.8805	.881	.882	.883	.885	.887
$10^3\,\mathrm{k/s^{-1}}$	$19.7 \pm .6$	$18.1 \pm .3$	$16.5 \pm .1$	$15.5 \pm .2$	$14.2 \pm .4$	$13.3 \pm .5$

The first row refers to the square difference summed, where the lowest value would in principle refer to the most accurate value (third entry from left). The second row refers to the A_∞ absorbance and the last to the corresponding rate constant with the most accurate believed at the stated units to be at $16.5 \pm .1$

Table 2 Data for the plot of Fig. 11 for reaction (i)

Result	Procedure	Poly. order	λ_∞	k_i
1	From expt	–	2, 050	1.7752×10^{-3}
2	Method 1	2	1, 134.3	3.3397×10^{-3}
3	Method 2	2	1, 130.23	3.347×10^{-3}
4	Sect. 2.0.5 R_α	2	1, 150.63	3.288×10^{-3}

Table 3 Data for the plot of Fig. 12 for reaction (ii)

Result	Procedure	Poly. order	λ_∞	k_{ii}
1	From expt	–	.8820	1.65×10^{-2}
2	Method 1	5	.8787	1.64×10^{-2}
3	Method 2	5	.8653	1.72×10^{-2}
4	Sect. 2.0.5 R_β	5	.89247	1.5497×10^{-2}

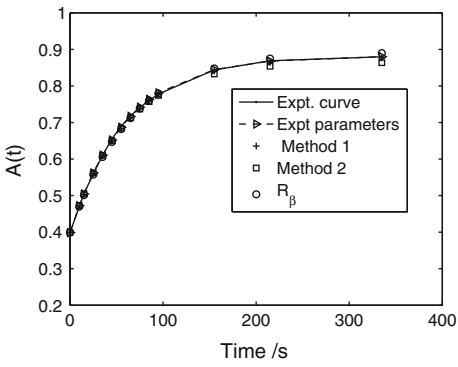

Fig. 12 The plots according to the k_{ii} and A_∞ values of Table 3

the reactions (i) and (ii) and the plots, we predict that reaction (i) if carried out under stringently controlled conditions, especially in determining λ_∞ would have a rate constant approximately $\sim 3.2 \times 10^{-3}\mathrm{min}^{-1}$ rather than the experimentally deduced $\sim 1.77 \times 10^{-3}\mathrm{min}^{-1}$ with $\lambda_\infty \sim 1{,}130$ units rather than 2,050 units since the NLA plots are a better fit than the one using the experimentally determined λ_∞. For reaction

(ii), we note a good fit for all the curves, that of the experiment, Khan's results and ours.

2.2 Evidence of varying kinetic coefficient k for reactions (i) and (ii)

Finally, what of direct methods that do not assume the constancy of k which was the case in the above subsections? Under the linearity assumption $x = \alpha\lambda(t)$, the rate law has the form $dc/dt = -k(t)(a - x)$ where $k(t)$ is the instantaneous rate constant and this form implies

$$k(t) = \frac{d\lambda/dt}{(\lambda_\infty - \lambda(t))} \tag{24}$$

If λ_∞ is known from accurate experiments or from our computed estimates, then $k(t)$ is determined; the variation of $k(t)$ could provide crucial information concerning reaction kinetic mechanism and energetics, from at least one theory recently developed for elementary reactions [14] *at equilibrium*; and for such similar theories [38] and experimental developments for very large changes in concentration, it may be anticipated that nonlinear methods would be used to accurately determine $k(t)$. Such an analysis could possibly also determine the so-called "reactivity coefficients" [14] that account for variations in k for homogeneously distributed reactants that would provide fundamental information concerning activation and free energy changes. However, since these coefficients pertain to the steady-state scenario where a precise relationship exists between the ratio of these coefficients and that of the activity, one might not expect to detect these coefficients for relatively minute concentration changes that occur in most routine chemical reaction determinations. On the other hand, the very preliminary results here seem to indicate transient variations belonging possibly to another class of phenomena; it could well be due to periodicity in the reactions where some of the "beats" detected—assuming no experimental error in the data—could be related to the time interval between measurements, that is, because the number of datapoints is restricted, only certain beats are observed in the periodicity. The assumption that the spectroscopic detector is not noisy relative to the magnitude of the experimental data and that it does not have significant periodic drift relative to a reference absorbance leads to the conclusion that some form of chemically induced periodicity might be present. It would be very interesting to increase the number of datapoints where the time interval between measurements is reduced and to analyze the different types of apparent frequencies that might be observed with different time intervals of measurement. From these observations, perhaps theories could be adduced on the nature of these presumed changes in the rate constant values over time, both for long and short time scales. Other rationalizations discussed in the conclusions of this work for the effect observed include improper mixing of the reactants that implies diffusion currents that is a possible cause for the convex shape of the curve.

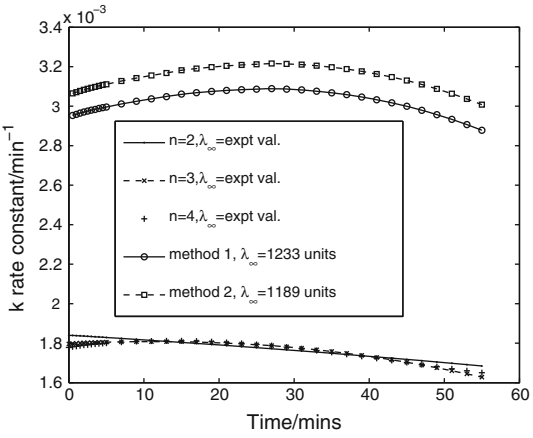

Fig. 13 Variation of k with time or concentration changes based on the experimental value λ_∞=2,050 units and the computations based on different polynomial degrees $n = 2, 3, 4$ and the computed λ_∞ values for Method 1 and Method 2 for fixed polynomial degree $n = 3$

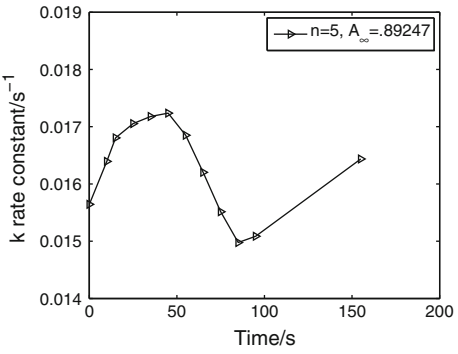

Fig. 14 An apparently periodically varying rate constant that settles to a higher value at larger time increments. A_∞ was the value taken from Method 1 above for polynomial order 5 for reaction (ii)

Reaction (i) results

Figure 13 refers to the computations under the assumption of first order linearity of concentration and the conductivity. Whilst very preliminary, non-constancy of the rate constants are evident, and one can therefore expect that another area of fruitful experimental and theoretical development can be expected from these results that incorporates at least some of the effects that has been postulated above.

Reaction (ii) results

To verify that the curious results are not due to minute fluctuations of the gradient, we plot the gradient $\frac{dl}{dt}$ of the curve fits for polynomial orders 1, 2, 4 and 5. Even for low orders, the fit is very good with no oscillations observed between lower and higher order polynomials for approximately the first 10 values of the kinetic data in Fig. 7. It was found that the lower order polynomials gave essentially the same results for the restricted domain where the gradients coincided with those of higher order.

The gradient drops to 0 at the long time $t \to \infty$ limit; on the other hand, the factor $\frac{1}{(\lambda_\infty - \lambda(t))}$ rises to infinity; so we might expect from these two competing factors various sinusoidal-like properties, or even maxima. The surprising result is shown in Fig. 14. It could be that the form (24) is not valid because no instantaneous value of the

rate constant can be defined. Also, it is not possible at this stage to definitively rule out the detector causing a sinusoidal variation due to periodic drift and instability. On the other hand, if we can rule out artifacts due to systematic instrument error, by comparing with other runs that do not use this instrument but which yields the same form of the plot then one must admit the possibility that a long-time cooperative effect involving coupling of the reactant molecules through the solvent matrix over the entire reaction chamber may take place. However, if the results are due solely to instrument error, then this method allows us to monitor the error fluctuations by taking a suitable weighted average. We note that reaction (ii) is relatively complex, involving many ionic species and some intermediate steps or reactions [33, pp. 414–416]. This fact, coupled with the cell setup where steady state temperature gradients might well exist, would lead to coupled processes described by irreversible thermodynamics, which could possibly explain such rate constant changes relative to the first order parametrization used here.

Comment: Barring artifacts, Figs. 13, 14 is consonant with two separate effects: (α) a long-time limit due to changes in concentration that alters the force fields and consequently the mean rate constant value (according to the theories in [14,38]) of the reaction as equilibrium is reached, and (β) possible transient effects due to collective modes of the coupling between the reacting molecules and the bulk solution as observed in the region between the start of the reaction and the long-time interval. In both reactions (i) and (ii), there appears a slight change in the rate constant value at time $t = 0$ and the values at the end of the experimental measured interval which may be due to the altered force fields that would change slightly the rate constant according to (α). On the other hand, there is a relatively slow and minute sinusoidal-like change in the rate constant that may be due to some cooperative effect, if no artifacts are implied; the interpolation with different polynomials leading to the same gradient seems to suggest that some type of collective behavior might be operating during the course of the reaction; if this is so then (β) would be a new type of phenomena that has not hitherto been incorporated into chemical kinetics research.

3 Results for reaction (iii) and (iv)

Two different methods are utilized to determine the reaction rate constants. The direct method utilizes determining the gradient k of the $d[A_1]/dt$ versus $[Q]$ curve of Eq. (2) by fitting the best straight line. Initial concentrations are not required, and the error in the gradient may be estimated from the mean least squares error of the end-points; define the mean square per point Δ^2 as $\Delta^2 = \sum_{i=1}^{n}(\bar{y} - y_i)^2/n$ where $\bar{y}$ is the linear optimized curve and y_i a datapoint within the range of measurement. Then for the range of datapoints $|X| = |Q|$ we estimate the error in the rate constant as $\Delta k = \sqrt{\Delta^2}/|X|$. For what follows below the first order rate constant for reaction (iii) is denoted k_{1d} derived from direct computation of the gradient of (2) whereas k_{1ls} denotes the rate constant as calculated by our least squares method (5). Similarly, for the seond order reaction (iv), k_{2d} denotes the rate constant derived directly from the gradient of the curve following Eq. (2) by fitting the best straight line and k_{2ls} is the second order rate

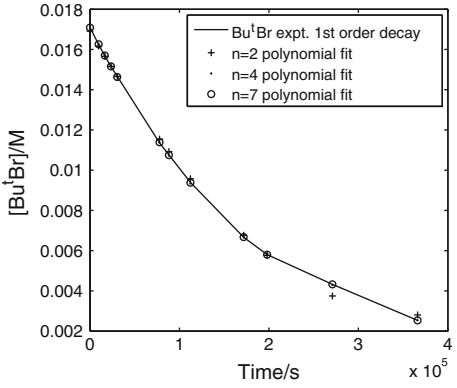

Fig. 15 The polynomial degree n for the orthogonal polynomial fit for the first order Bu^tCl reaction (iii) where there is near coincidence for $n = 4, 5, 6, 7$

constant from the *least squares minimization* technique of (5). A detailed description follows below.

The general 1st and 2nd order equations We state the standard integrated forms below as a reference that requires specification of initial concentrations in order to contrast them to the methods developed here. In the standard methodology, the first order rate constant k_1 is determined from

$$k_1 = \frac{1}{t} \log_e \{b(b - x)\} \tag{25}$$

and the second order rate constant k_2 is determined from

$$k_2 = \left[\frac{1}{t(a - b)}\right] \log_e \frac{b(a - x)}{(b - x)} \tag{26}$$

where these expressions are given in [35, p. 2063] and these equations were used by those that ran reactions (iii) and (iv) to determine the rate constants, where a and b are the initial concentration terms at $t = 0$ and x is the extent of reaction and where by hypothesis k_1 and k_2 are constants for all times t.

3.1 Reaction (iii) first order details

Figure 15 is a plot of the various orthogonal polynomial order fits. The $n = 2$ order is rather poor but higher orders all coincide with the experimental points. And for $n > 2$, we find that the gradient curves coincide within a certain range where [A] > 0.005M. If in fact the order is 1 or unity, a plot of [Å]versus[A] would be entirely linear. Figure 16 depict these plots, where some linearity is observed for [A] > 0.005 M.

Figure 16 shows a coincidence of the rate curves for order $n = 5$–7 above [A] = 0.005 M. It may be therefore inferred that for at least $n > 5$, and for [A] > 0.005 M, the gradient represents the rate constant. The inaccuracy for very low

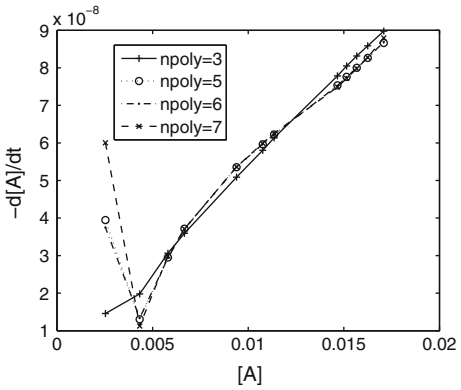

Fig. 16 A plot of the rate of decomposition of $Bu^tBr(\equiv \dot{A})$ versus A where [A] refers to the molar concentration of Bu^tBr according to the kinetic data published in [34, Table IX] for reaction (iii)

Table 4 Results for the first order Bu^tBr reaction (iii) neglecting last datapoint for calculating the mean rate constant k

n	k_{1d}/s^{-1}	k_{1ls}/s^{-1}	Est. error in k	Abs. dev. in n
2	5.038689×10^{-6}	4.881742×10^{-6}	4.164406×10^{-7}	0.000151
3	5.374684×10^{-6}	5.307609×10^{-6}	8.129860×10^{-8}	0.000073
4	5.053045×10^{-6}	5.047342×10^{-6}	3.541633×10^{-7}	0.000034
5	5.398782×10^{-6}	5.181527×10^{-6}	2.772767×10^{-7}	0.000014
6	5.393767×10^{-6}	5.184763×10^{-6}	2.723767×10^{-7}	0.000013
7	5.500610×10^{-6}	5.187774×10^{-6}	3.028407×10^{-7}	0.000014

concentrations may be explained by reference to Fig. 15. The experimental curve is parametrized as

$$[\mathrm{A}] = \sum_{i=1}^{n_r} h_i t^i \tag{27}$$

The time parameter is very large at low concentrations ($>3.5\times10^5$ s) of Bu^tBr; the h_i values would be small and the uncertainties in the reactant concentration relatively high; this explains the large scatter in the gradient values at low concentrations. We therefore ignore the first two values of [A] at low concentrations and focus on the gradients for points of coincidence of the different polynomial curves in in Fig. 16. The results are shown in Table 4. The linear fit in this specified range yields k_{1d}. The absolute root mean squared deviation per datapoint of Fig. 15 is listed in the last rhs column of Table 4 where the best fit is in the range n =5–7. The average k_{1d} value taking into account the error estimate is $(5.4 \pm 0.5) \times 10^{-6}s^{-1}$, which is close to the $(5.22 \pm 0.3) \times 10^{-6}s^{-1}$ of the experimentalists.

The results from the literature for this first order reaction [34, Table IX, p. 2071] using Eq. (25) has a mean value of 5.22×10^{-6} and for the 12 datapoints determined, k varied with range $(5.04–5.48)\times10^{-6}$ in appropriate dimensions. The results

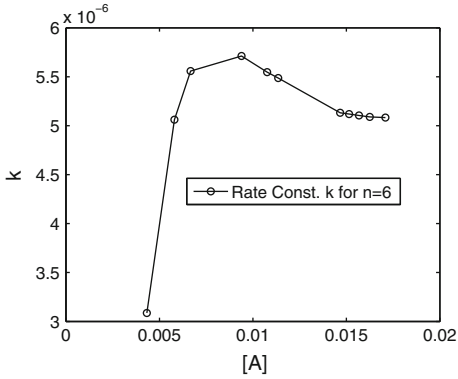

Fig. 17 The direct calculation of the change of the rate constant with concentration [A] = [Bu^{t}Br] directly from the published experimental data [34, Table IX] for reaction (iii)

as computed according to our methods in Table 4 show the absolute deviation per point to be quite small, and Fig. 15 shows some plots. The gradient of the curves are graphed for various n in Fig. 16. The linear fit in this specified range yields k_{1d}. The absolute root mean squared deviation per datapoint of Fig. 15 is listed in the last rhs column of Table 4 where the best fit is in the range n =5–7. The average k_{1d} value taking into account the error estimate is $(5.4 \pm 0.5) \times 10^{-6}\text{s}^{-1}$ which is close to the $(5.22 \pm 0.3) \times 10^{-6}\text{s}^{-1}$ of the experimentalists. For the same regime, (5) is used to compute k_{1ls} listed in the 3rd column. For n =5–7, $k_{ls} = 5.18 \times 10^{-6}\text{s}^{-1}$ which is exceptionally close to the experimental determination mentioned above based on the integrated equation (25) requiring initial concentrations.

Lastly, (3) is used to compute the instantaneous rate constant shown in Fig. 17. We note that a maximum is formed before a drop at lower concentrations. Again, the convex form with a maximum is evident here as for reactions (i)–(ii).

3.2 Reaction (iv) second order details

The pioneer experimentalists had decided a *priori* that the NaOEt–iso-PropylBr (Pr^{i}Br) reaction was second order and therefore did not independently measure the NaOEt and the Pr^{i}Br concentrations as shown in Fig. 18. Such a setting introduces a larger degree of scattering even if the rate order is known a *priori* to be the appropriate one; the scattering is evident in the rate constant curve of Fig. 1. The orthogonal polynomial fit is very good for $n > 3$ in Fig. 18. The gradient curve of Fig. 19 shows a coincidence of points for polynomial order $n > 3$ except for the measurement at the lowest concentrations, for the same reasons as given for reaction (iii). Figure 20 is a close-up of the rate versus [A][B] curve where the first 2 points show significant scatter. We ignore the first 3 points of lowest concentrations in our calculations for k_{2d} and k_{2ls} for different polynomial orders n; k_{2d} is the rate constant by linear least squares fit to each of the curves of Fig. 19 of d[A]/dt versus [A][B] for different polynomial orders n and k_{2ls} is the rate constant calculated according to (5). The results are presented in Table 5. In Table 5, the value of k_{2d} is remarkably constant for n =4–7, in keeping with the curves of Fig. 19 that are coincident for the selected

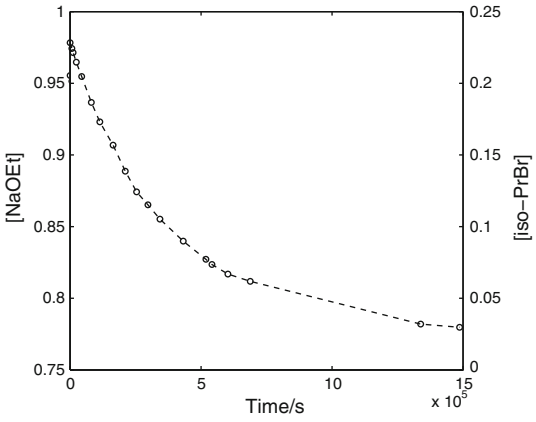

Fig. 18 The experimental decay *curve* for the NaOEt–iso-PropylBr ($Pr^i Br$) reaction [35, Table VII, p. 2064] for reaction (iv)

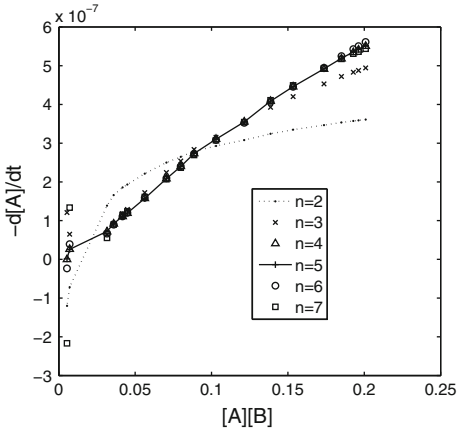

Fig. 19 The rate *curve* for reaction (iv) shows that the polynomial order n =2–3 is too low to fit the changes of gradient. The other *curves* of higher order all coincide exact for very large time values or low reactant concentrations. The average gradient is calculated by ignoring these values that are off-scale.[[A] ≡ [NaOEt]] and [[B] ≡ [iso-PropylBr]] in molar concentration units

concentration ranges where we have $k_{2d} = (2.80 \pm .07) \times 10^{-6}\,\mathrm{M^{-1}\,s^{-1}}$ which is very close also to the computed k_{2ls} values, where the average value may be written $k_{2ls} = (2.83 \pm .05) \times 10^{-6}\,\mathrm{M^{-1}\,s^{-1}}$.

The experimental results for this second order reaction [35, Table VII, p. 2064] using equation (26) has a mean value of $2.88 \times 10^{-6}\,\mathrm{M^{-1}\,s^{-1}}$ ($2.95 \times 10^{-6}\,\mathrm{M^{-1}\,s^{-1}}$ if solvent expansion is taken into account according to an extraneous theory), and for the 19 datapoints determined , k varied within the range $(2.76-2.96)\times 10^{-6})\,\mathrm{M^{-1}\,s^{-1}}$. Figure 1 graphs the instantaneous rate constant for reaction (iv) for the concentration ranges used for calculating k_{2d} and k_{2ls}. Again a semi-sinusoidal shaped curve is observed. There is evident scatter in this graph which may be attributed to the fact that [A] and [B] are completely correlated and there is no possibility of random cancellations due to independent measurement of both [A] and [B]. The form of the curve is as for reaction (iii) in Fig. 17 *and* as for reaction (ii) in Fig. 14 if we ignore the low concentration value as having a large scatter at about $t = 150\,\mathrm{s}$. Even the ambiguous

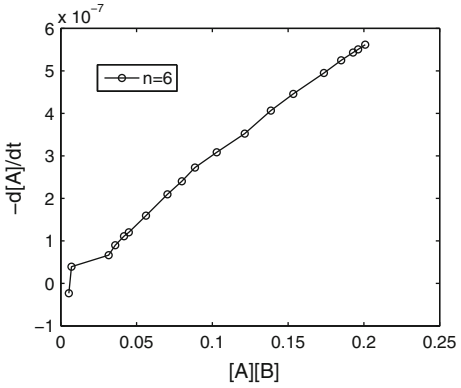

Fig. 20 Close-up of the rate *curve* for reaction (iv) with reactant product concentration for polynomial fit $n = 6$. The last 3 lowest product concentration points are ignored in the rate averaging to determine the rate constant

Table 5 Results for the second order Pr^iBr–NaOEt reaction (iv) neglecting the last 3 datapoints that are discontinuous for calculating the rate constants k_{2d} and k_{2ls}

n	$k_{2d}/M^{-1}s^{-1}$	Error Δk_{2d}	$k_{2ls}/M^{-1}s^{-1}$
2	1.251043×10^{-6}	1.189216×10^{-7}	2.180891×10^{-6}
3	2.142702×10^{-6}	8.845014×10^{-8}	2.654936×10^{-6}
4	2.818337×10^{-6}	6.850636×10^{-8}	2.829915×10^{-6}
5	2.822939×10^{-6}	6.600369×10^{-8}	2.833440×10^{-6}
6	2.876573×10^{-6}	6.613089×10^{-8}	2.853618×10^{-6}
7	2.770475×10^{-6}	7.707235×10^{-8}	2.823186×10^{-6}

reaction (i) shows a shallow convex shape, as with all the rest. Figure 21 is a pallet for the 4 diverse reactions (i)–(iv) of different orders reported by different sources all depicting the same general form which is suggestive of some type of overall "chemical momentum" effect. The data for reaction (ii) was determined over 50 years apart from (iii) and (iv), and all these by prominent persons, especially Ingold and co-workers who were amongst the best kineticists of the twentieth century, in addition to the fact that the Ingold group were responsible for elucidating and defining the SN1, SN2, E1 and E2 reactions in organic chemistry. It seems that all these reactions depict a transient and long-ranging coupling phenomena hitherto unnoticed due to traditional analysis that uses integrated rate law expressions with the presupposition of invariant rate constants, which is also built into current statistical mechanics theories. There could be at least two possible separate effects that could contribute to the above observations:

(a) independently of the initial concentrations, one observes a rise in the rate constant before falling when the reactant concentration falls. Hence if we started a reaction at the midpoint concentrations close to the peak rate constant value in the reaction runs for reactions (ii)–(iv), then the rate constant profile will show a form similar to those shown here, except the peak rate constant will shift to lower concentrations, at least at a concentration less than the concentration at the commencement of the reaction. This possibility suggests some type of "chemical momentum" which is a long-ranging coupling phenomena that current statistical

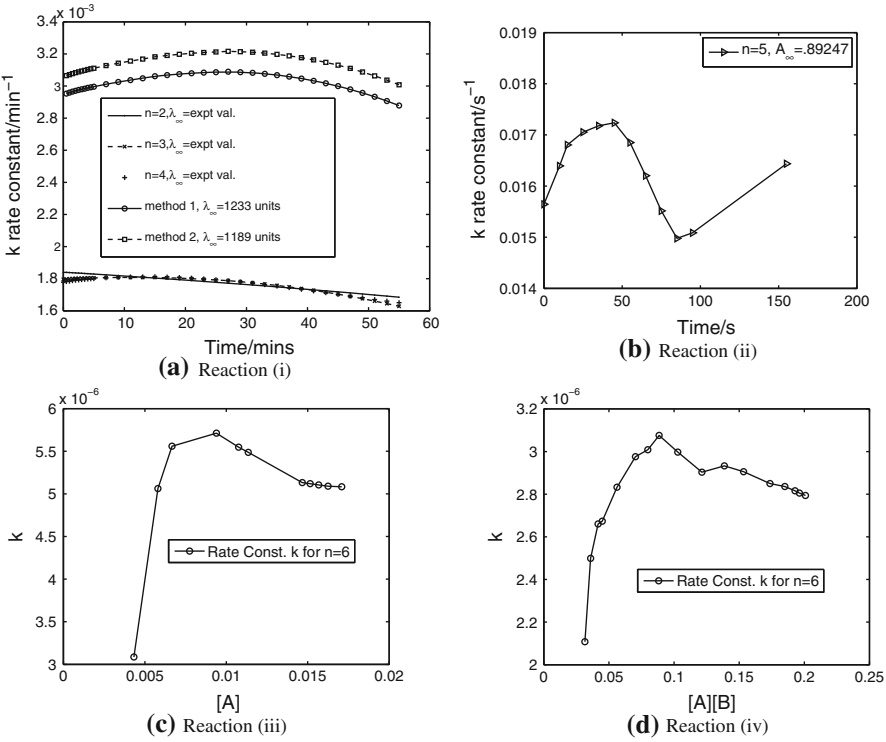

Fig. 21 Collation of change of rate constants with concentration and time for reactions (i)–(iv)

mechanical theories are not able to account for. Obviously this scenario admits the possibility of hysteresis behavior

(b) the rate constant is simply a function of reactant and product concentrations as outlined for instance in [14] and no hysteresis behavior exists. This possibility would encompass imperfect mixing of the reactant components at the commencement of the reaction, so that time dependent diffusion and structural readjustment factors would be involved in explaining this possibility.

Currently, mainstream statistical mechanical theories do not have a quantum or classical description of (a) and (b) above.

Reality would probably be described by predominantly either (a) or (b) above with a possibility of the other playing a minor role in the final effect.

More careful experiments under stringent conditions need to be performed to :

α. verify the existence of this effect by using other methods just in case the polynomial method has a property that induces a maximum in the gradient at approximately the midpoint of the domain range under investigation

β. determine which of the two (a) or (b) above is the preponderant effect.

4 Conclusions

The differential methods developed here yield results for the average rate constant that is consistent and close in value to the traditional integrated law expression for 3 reactions whose rate constants were determined with precision by reliable and prominent kineticists, implying that the methods developed here are robust. Based on reproducibility of the method in relation to the standard protocol, we further test the differential methods for the ambiguous reaction (i) with regard to the inaccurate total reactant concentration (reflected in λ_∞) and we showed that the rate constant can be determined without such data. Since much science refers to systems whose key variables are not controllable, as in astrophysical measurements and in forensics and archaeological studies, these methods could prove useful for analysis in these areas for reactions to arbitrary order.

All the reactions studied with different orders and mechanisms within the polynomial optimization method all show some type of "chemical rate constant momentum" effect in that there is a gradual acceleration in the rate over time initially followed by a sharp decrease as the reactants deplete. This observation appears to be novel. Two independent factors might contribute to this effect:

(A.) the transient coupling of thermodynamical force gradients with flows and species concentrations and molecular orientation that leads to the observed profile
(B.) the rate constant is a second order function of the reactant and product concentration according to [14]. That theory was based on evidence from *equilibrium* MD simulation of a chemical reaction.

Stringently controlled repeated experimentation is required to determine the relative contributions of (A.) and (B.) above. If a semi-sinusoidal profile is observed for different initial concentrations that covers the range of the concentration profile of a reference reaction of exactly the same type which also exhibits a semi-sinusoidal profile, then (A.) is the predominant mechanism which causes hysteresis behavior, whereas if the resulting profile of the experiments leads to a truncated semi-sinusoidal curve of the reference profile beginning at the initial concentration of the experimental run, the (B.) is the major effect. There is of course the possibility of a combination of effects (A.) and (B.) to varying degrees. Both effects have not been anticipated in current kinetic theories, which implies that these effects in themselves constitutes one area for further investigation.

Whilst the main purpose of this work is not to provide physical explanations, we suggest that the resulting curves in Fig. 21 can be explained by introducing at least 3 contributing factors or processes in real time. The first (f1) involves the fact that the reactants are initially separated, and the molecules must diffuse homogeneously before they can begin to interact. The second process (f2) involves reactant interaction with the solvent matrix, which would impede the reactive interactions and also conceivably raise the activation energy relative to unbounded reactants and lastly (f3) describes the product solvent matrix interaction, which is probably not too significant for the typical reactions studied here. At the initial stage of the reaction, there is minimal solvent reactant interaction which would result in the caging of the reaction active sites and so the reaction is diffusion limiting; within a certain time scale, the mutual

diffusion of reactants would allow for more reactant-reactant interactions, leading to an apparent increase in the rate constant; with the progress in time, however, the caging of reactants due to (f2) would increase the effective activation energy and hence lower the value of the rate constant which explains the precipitous drop at large time values; process (f3) might prevent in some cases the back reaction due to the breakup of the product to reactant molecules, and it may moderate (f2) by liming the number of active solvent interaction with the reactant molecules. One might expect (f1) to cause the rise in the rate constant, and (f2) the lowering, leading to the convex maximum observed in all the reactions due to these competing processes. Factors (f1)–(f3) together would result in phenomena (A.) above. Conventional kinetics, modeled after ideal situations of homogeneity, is not able to account for these fine second order details in the change in the reaction rate during the course of the reaction. Even in the homogeneous case, such as a reactive system in thermodynamical equilibrium, it was found that the rate constant is a well-defined function of the reactant and product concentrations, but this contribution to the changes found here is probably of second order for the typical reactions mentioned here because of the relatively low concentrations of the active species within an inert solvent matrix which did not feature in the simulation studies.

The results presented here provides alternative developments based on NLA that is able to probe into the finer details of kinetic phenomena than what the standard representations allow for, especially in the the areas of changes of the rate constant with the reaction environment. NLA can also determine average rate constant values without λ_∞ being known or determined. Even with the assumption of invariance of k, one can always choose the best type of polynomial order that is consistent with the assumption, and it appears that the initial concentration as well as the rate constant seem to feature as global properties based on the polynomial expansion, since taking limits as the time parameter $t \to 0$ yields information about the rate constant and initial concentrations. It should be noted that the examples chosen here were first order ones; the methods are general and they pertain to any form of rate law where the gradients and forms can be curve-fitted and the form of the equations optimized as in Sect. 2.0.5. One other research area that may be investigated is the possibility of reactions of fractional order; elementary reactions are by nature of integer order. Is there a method that can reduce them to fractional order if the rate constant is indeed in part a weak function of the reactant concentrations?

Acknowledgments This work was supported by University of Malaya Grant UMRG(RG077/09AFR) and Malaysian Government grant FRGS(FP084/2010A).

References

1. R.K. Pathria, *Statistical Mechanics*, 2nd edn. (Butterworth-Heinemann, Oxford, 2001), paperback
2. J.K. Baird, Y.W. Kim, Fluctuation-dissipation theorem for chemical reactions near a critical point. J. Phys. Chem. A **107**, 10241–10242 (2003)
3. L.Y. Chen, Nonequilibrium fluctuation-dissipation theorem of brownian dynamics. J. Chem. Phys. **129**, 144113-1–144113-4 (2008)
4. G.L. Hofacker, Later developments of Eyring's ideas of the activated complex. Int. J. Quantum Chem. **3**(13/18), 33–37 (1969)

5. Y. Zhou, X. Zhuang, Robust reconstruction of the rate constant distribution using the phase function method. Biophys. J. **91**(11), 4045–4053 (2006)
6. E.E. Escultura, Personal website url: users.tpg.com.au/pidro/problem.html
7. E.E. Escultura, Qualitative model of the atom, its components and origin in the early universe. Nonlinear Anal. Real World Appl. **11**, 29–38 (2010)
8. E.E. Escultura, The flux theory of gravitation XVII. The new mathematics and physics. Appl. Math. Comput. **138**, 127–149 (2003)
9. E.E. Escultura, THE GRAND UNIFIED THEORY A SUMMARY. The above essay is featured in the Free Library depository with the url: http://www.thefreelibrary.com/THE+GRAND+UNIFIED+THEORY+A+SUMMARY-a01074003661
10. E. Escultura, T.G. Bhaskar, V. Lakshmikantham, S. Leela, Revisiting the hybrid real number system. Nonlinear Anal. Hybrid Syst. **3**, 101–107 (2009)
11. E.E. Escultura, Turbulence: theory, verification and applications. Nonlinear Anal. **47**, 5955–6966 (2001)
12. E.E. Escultura, The grand unified theory (GUT I). The solution of the gravitational n-body problem. Nonlinear Anal. **30**(8), 5021–5032 (1997)
13. E.E. Escultura, V. Lakshmikantham, S. Leela, *The Hybrid Grand Unified Theory*. (Elsevier Science Ltd, Atlantis, Paris, 2009)
14. C.G. Jesudason, The form of the rate constant for elementary reactions at equilibrium from MD: framework and proposals for thermokinetics. J. Math. Chem. **43**, 976–1023 (2008)
15. P. Moore, Analysis of kinetic data for a first-order reaction with unknown initial and final readings by the method of non-linear least squares. J. Chem. Soc. Faraday Trans. I **68**, 1890–1893 (1972)
16. E.A. Guggenheim, On the determination of the velocity constant of a unimolecular reaction. Philos. Mag. J. Sci. **2**, 538–543 (1926)
17. W.D. Johnson, M.C. Maltby, The application of polynomial expressions to determine the initial concentrations and rate constants of chemical reactions. Aust. J.Chem. **24**, 2417–2420 (1971)
18. E.S. Swinbourne, Method for obtaining the rate coefficient and final concentration of a first-order reaction. J. Chem. Soc. **473**, 2371–2372 (1960)
19. E.S. Swinbourne, Determination of the rate coefficient and final concentration of a reaction of order n. Aust. J.Chem. **16**(1), 170–173 (1963)
20. R.C. Williams, J.M. Taylor, Computer calculations of first-order rate constants. J. Chem. Educ. **47**(2), 129–133 (1970)
21. N.H. Lajis, M.N. Khan, Kinetic demonstration of chemospecific reactions involving salicylate esters and amines. J. Chem. Educ. **70**(10), A264–A271 (1993)
22. M.J.J. Holt, A.C. Norris, A new approach to the analysis of first-order kinetic data. J. Chem. Educ. **54**(7), 426–428 (1977)
23. W.E. Wentworth, Rigorous least squares adjustment. Application to some non-linear equations, II. J. Chem. Educ. **42**(3), 162–167 (1965)
24. W.E. Wentworth, Rigorous least squares adjustment. Application to some non-linear equations, I. J. Chem. Educ. **42**(2), 96–103 (1965)
25. J.J. Houser, Estimation of A_∞ in reaction-rate studies. J. Chem. Educ. **59**(9), 776–777 (1982)
26. J.E. Cortés-Figueroa, D.A. Moore, Using a graphing calculator to determine a first-order rate constant when the infinity reading is unknown. J. Chem. Educ. **79**(12), 1462–1464 (2002)
27. K.B. Wiberg, Use of computers, in *Techniques of Chemistry*, ed. by E.S. Lewis, vol. VI of *Investigation of rates and mechanisms of reactions*, Chap. XIII. Part 1 General considerations and Reactions at Conventional Rates. (Wiley-Interscience, 1974), pp. 741–776
28. D.F. De Tar, LSKIN1, in *Computer Programs for Chemistry*, vol. I, Chap. 6, ed. by D.F. De Tar. Fortran Program listing with brief theoretical explaination (W. A. Benjamin, New York, Amsterdam, 1969), p. 126
29. D.F. De Tar, LSKIN2, in *Computer Programs for Chemistry*, vol. 4, Chap. 1, ed. by D.F. De Tar (Academic Press, New York and London, 1972), p. 1. The chapter describes a method based on expansion of integrated rate equations for second order reactions that give estimates of the rate constant and initial concentrations
30. X. Zhang, J.M. Ajello, Y.L. Yung, Atomic carbon in the upper atmosphere of Titan. Astrophys. J. **708**, L18–L21 (2010)
31. M.B. McElroy, J.C. McConnell, Atomic carbon in the atmospheres of Mars and Venus. J. Geophys. Res. **76**(28), 6674–6690 (1971)

32. C.A. Barth, C.W. Hord, J.B. Pearce, K.K. Kelly, G.P. Anderson, A.I. Stewart, Mariner 6 and 7 ultraviolet spectrometer experiment: upper atmospheric data. J. Geophys. Res. **76**, 2213–2217 (1971)
33. M.N. Khan, *Micellar Catalysis*, vol. 133 of *Surfactant science series*. (Taylor & Francis, Boca Raton, 2007) Series Editor A.T. Hubbard
34. M.L. Dhar, E.D. Hughes, C.K. Ingold, 421. Mechanism of elimination reactions. Part XI. Kinetics of olefin elimination from tert.-butyl and tert.-amyl bromides in acidic and alkaline alcoholic media. J. Chem. Soc., 2065–2072 (1948)
35. M.L. Dhar, E.D. Hughes, C.K. Ingold, 420. Mechanism of elimination reactions. Part X. Kinetics of olefin elimination from isopropyl, sec.-butyl, 2-*n*-amyl, and 3-*n*-amyl bromides in acidic and alkaline alcoholic media. J. Chem. Soc., 2058–2065 (1948)
36. S. Yakowitz, F. Szidarovsky, *An Introduction to Numerical Computations* (Maxwell Macmillan, New York, 1990)
37. W.H. Press, S.A. Teukolsky, W.T. Vetterling, B.P. Flannery, *Numerical Recipes in C—the Art of Scientific Computing*, 2nd edn. (Cambridge University Press, Cambridge, 2002)
38. C.G. Jesudason, An energy interconversion principle applied in reaction dynamics for the determination of equilibrium standard states. J. Math. Chem. (JOMC) **39**(1), 201–230 (2006)